ORGANOMETALLICS

Article

pubs.acs.org/Organometallics

Iron and Manganese Complexes of 2-Carbonyl Pyrrolyls: Scorpionate Sandwich Anions and Extended Structures

Lihong Li,[†] Guy J. Clarkson,[†] Martin R. Lees,[‡] Suzanne E. Howson,[†] Sze-yin Tan,[†] Scott S. Turner,[§] and Peter Scott*[,†]

[†]Department of Chemistry and [‡]Department of Physics, University of Warwick, Gibbet Hill Road, Coventry, CV4 7AL, U.K.
[§]Department of Chemistry, University of Surrey, Guildford, Surrey GU2 7XH, U.K.

Supporting Information

ABSTRACT: Attempts to synthesize complexes of Fe and Mn(II) with 2-amidopyrrolyl ligands (N−O) were unsuccessful, and only small amounts of the trivalent tris complexes M(N−O)$_3$ were detected, although unusually in the case of Fe(III) a *fac* structure is observed. In contrast the 2-benzoylpyrrolyl systems give M(II) complexes, and in all instances thus far where Na^+ is present, a scorpionate *fac*-$[M^{II}(N{-}O)_3]^-$ unit self-assembles into sandwich anions $[M^{II}(N{-}O)_3Na(O{-}N)_3M^{II}]^-$ in which the central metal is efficiently encapsulated by interdigitation of the aryl units. Extended structures are readily made through the use of a 2-(4-pyridinoyl)pyrrolylamide ligand. When Li^+ is used, the scorpionate ligand is not assembled, and instead [M(N−O)$_2$] units give rhombic 2D grids. The Fe system displays spin-crossover at 120 K.

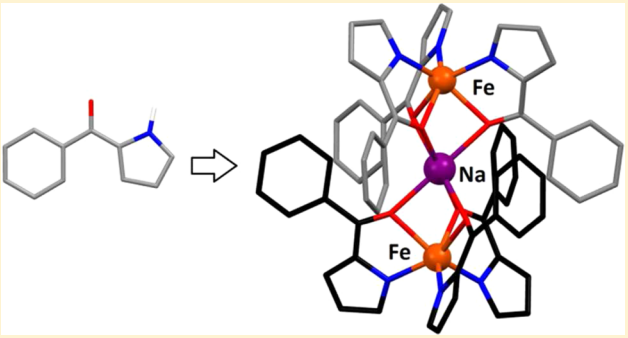

INTRODUCTION

Lappert was famed for his exploration of delocalized chelate and multidentate ligands.[1−3] His work was driven in part by the search for ancillary ligands that might rival the cyclopentadienyls in terms of their ability to support structures and reactivity, and we now take for granted many of such advances that were made. Among these ligands were the *β*-diketiminates, or NacNac, ligands,[4−9] which have become very important in modern organometallic chemistry.[10,11] Today, a great number of chelate amido ligands supported by conjugated donor atoms are used in organometallic reactions and catalysis,[12−22] and this research owes a great deal to fundamental studies by Lappert.

We considered the possibility that pyrrole derivatives such as HL$^{1-3}$ incorporating a *β*-carbonyl unit might provide an interesting ligand set, noting Okuda's related pyrrolide-imine system, which furnished remarkably active ethylene polymerization catalysts.[23] A few reports of such complexes have appeared.[24,25] Gambarotta performed a vanadium-mediated Aldol coupling of acetylpyrroles, leading to dinuclear olefin polymerization catalysts,[26] and a ruthenium compound catalyzed the Murai reaction.[27] A cytotoxic Pt complex has been reported.[28] Love demonstrated that tripodal pyrrolylamides provide inner- and outer-sphere coordination environments.[29]

In this study, the three ligands of Chart 1 were chosen, as they might provide relatively hard (**L**^{1}) and soft (**L**^{2}) donor sets and the possibility of creation of extended structures (**L**^{3}). The complexes formed at Mn and Fe include conventional trischelates, new trimetallic sandwich-like structures, and extended 2D lattice architectures, and there is very good control over the product through choice of ligand and reagents.

Chart 1. Pyrrole-2-carbonyl Derivatives Used in This Work

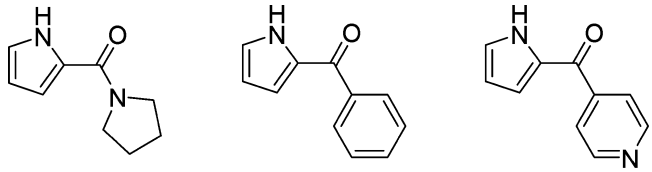

RESULTS AND DISCUSSION

Synthesis of Proligands. The 2-pyrrolylamide HL^1 was prepared readily using a literature route from commercially available 2-trichloroacetylpyrrole and pyrrolidine.[30] Phenyl pyrrolyl ketone HL^2 was made[31] via 1-benzoylmorpholine, which was converted with $POCl_3$ to the Vilsmeier reagent before treatment with pyrrole. The 4-pyridyl analogue HL^3 was synthesized by a Friedel−Crafts reaction between isonicotinoyl chloride and pyrrole using $AlCl_3$.

Special Issue: Mike Lappert Memorial Issue

Received: November 30, 2014
Published: May 15, 2015

DOI: 10.1021/om501218a
Organometallics 2015, 34, 2543−2549

Complexes of L^1. Reactions of NaL^1 (prepared *in situ* using NaH) with MCl_2 (M = Mn, Fe) in THF gave gray suspensions, from which a few crystals of tris complexes of the trivalent metals $[ML^1_3]$ (M = Mn, Fe) were isolated. Presumably the formation of this minor product is a result of disproportionation. No other products were isolated.

The structure of $[MnL^1_3]$ (Figure 1a) has a *mer* configuration, as is most commonly observed for trischelates

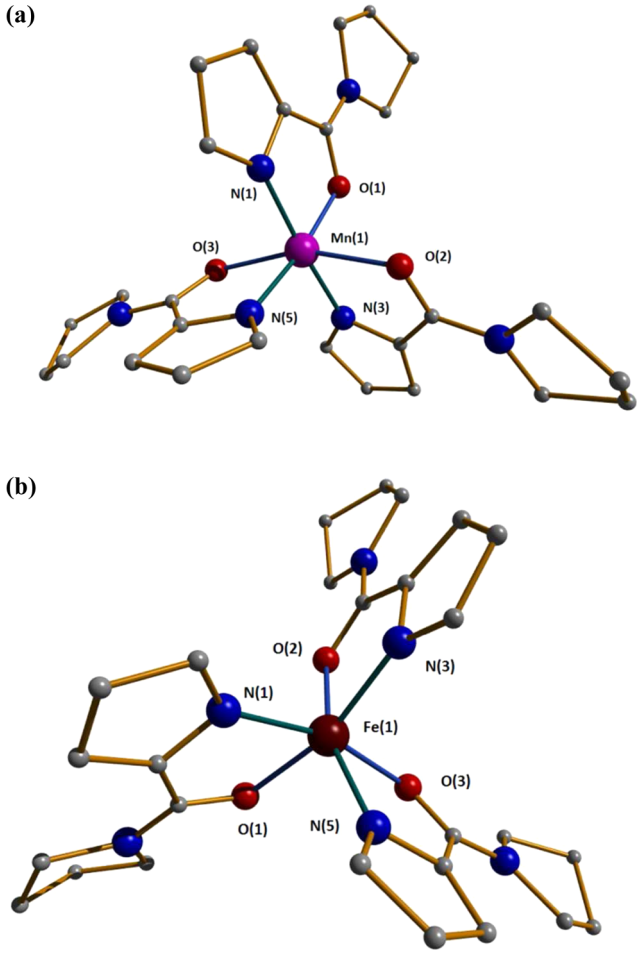

Figure 1. Molecular structures with selected bond lengths (Å) and angles (deg): (a) *mer*-$[MnL^1_3]$ Mn(1)−O(1) 1.959(4), Mn(1)−N(1) 1.960(5), Mn(1)−N(5) 1.972(5), Mn(1)−N(3) 1.991(5), Mn(1)−O(2) 2.206(4), Mn(1)−O(3) 2.214(4), O(1)−Mn(1)−N(5) 171.01(18), O(2)−Mn(1)−O(3) 160.27(14), N(1)−Mn(1)−N(3) 174.5(2); (b) *fac*-$[FeL^1_3]$ Fe(1)−N(3) 2.0404(19), Fe(1)−N(5) 2.0436(18), Fe(1)−N(1) 2.0489(18), Fe(1)−O(2) 2.0520(14), Fe(1)−O(3) 2.0686(14), Fe(1)−O(1) 2.0850(14), N(5)−Fe(1)−O(2) 161.05(7), N(1)−Fe(1)−O(3) 163.51(7), N(3)−Fe(1)−O(1) 164.72(7).

of unsymmetrical bidentate ligands for statistical reasons,[32] while $[FeL^1_3]$ (Figure 1b) is *fac*. An analysis of intermolecular contacts in the crystal did not indicate why this unusual structure has been adopted, there being for example no evidence of intermolecular chelation of the three O atoms.[33] As we will see, however, this *fac* structure is prevalent in the L^2 and L^3 systems. In other respects, the bond lengths and angles of $[ML^1_3]$ are within normal limits,[34] the five-membered chelate rings leading to structures close to octahedral.

Complexes of L^2. The observation of spontaneous oxidation to M(III) complexes for the amide ligand L^1 prompted us to investigate the behavior of the benzoyl derivative L^2.

The reaction of anhydrous $FeCl_2$ with NaL^2 in THF afforded a deep red solution, from which red single crystals of the Fe(II) salt complex $[Na(THF)_6][(FeL^2_3)Na(L^2_3Fe)]$ were collected (32%). While there was some disorder, the structure was refined satisfactorily.

While the complex cation (Figure 2) is composed conventionally of a sodium ion surrounded by six THF molecules, the

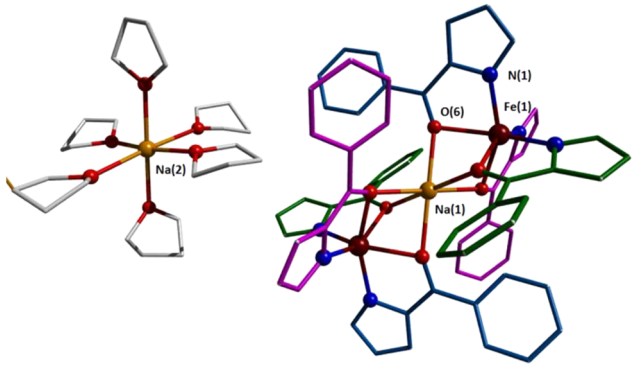

Figure 2. Structure of $[Na(THF)_6][(FeL^2_3)Na(L^2_3Fe)]$ showing the complex cation and anion with minor disorder removed and the L^2 ligand C atoms colored for clarity. Selected bond lengths (Å): Fe(1)−N(1) 2.094(4), Fe(1)−O(6) 2.277(4), Na(1)−O(6) 2.323(4). Selected bond angle (deg): Fe(1)−Na(1)−Fe(1) 180.

anion is an unusual trimetallic sandwich-like species. Two anionic *fac*-$(Fe^{II}L^2_3)$ units—similar in structure to the Fe^{III} species of Figure 1b—are coordinated via three O atoms each to the central Na cation. The amido N−Fe distances are slightly longer than in the Fe^{III} species as expected, and the Fe−O distance of 2.277(4) Å is substantially longer as a result of the O atom bridging to the central Na(1). The N−Fe−N angles of 90−93° in the monometallic Fe^{III} structure have opened up to 101.39(9)° here, also as a result of chelation to sodium. The space-filling views of the complex anion shown in Figure 3 indicate how the phenyl groups are interdigitated.

The nature of this unusual anion, comprising two high-spin Fe(II) centers at a distance of ca. 6.3 Å, prompted us to briefly investigate the magnetic properties. From 300 to 100 K, the value of $\chi_M T$ is nearly constant at 3.67 cm^3 K mol_{Fe}^{-1}, higher than that expected for free high-spin Fe(II) (3.001 cm^3 K mol^{-1}, g = 2.00) as a result of spin−orbit contributions (generally $g > 2.00$)[34] but in agreement with the value of C = 3.761 cm^3 K mol^{-1} from Curie−Weiss fitting (see SI), from which a value of g = 2.20 was derived. On lowering the temperature, $\chi_M T$ gradually fell, due to zero field splitting, and, as expected, the Fe^{II} centers are coupled antiferromagnetically (Θ = −3.37 K).

The reaction of $MnCl_2$ with NaL^2 in THF gave a yellow solution from which crystals could not be obtained directly. Recrystallization of the solid product from Et_2O yielded yellow blocks (52%). A partially resolved crystal structure revealed a very similar structure to the Fe^{II} complex, and the formula $[Na(THF)_6][(MnL^2_3)Na(L^2_3Mn)]$ was confirmed by microanalysis.

For this compound, while $\chi_M T$ fell from 4.493 cm^3 K mol^{-1} at room temperature to 4.330 cm^3 K mol^{-1} at 14 K, indicating weak antiferromagnetic exchange between Mn(II) ions (Figure 4), the value then increased rapidly to a maximum of ca. 5.1

DOI: 10.1021/om501218a
Organometallics 2015, 34, 2543−2549

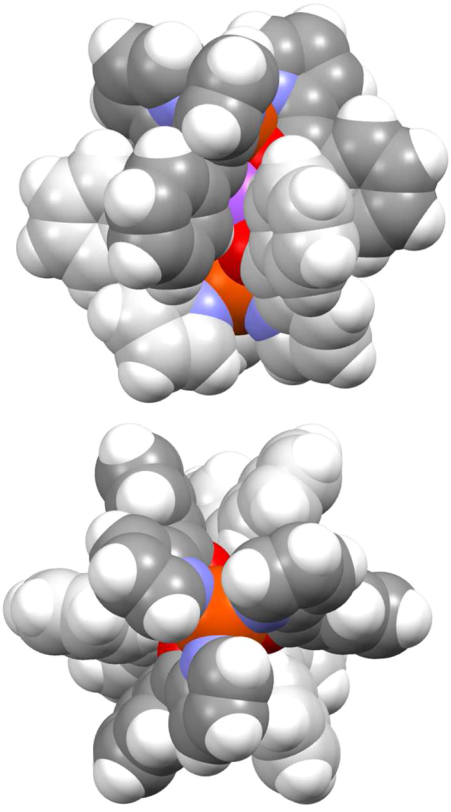

Figure 3. Interdigitation of $(FeL^2_3)^-$ in $[(FeL^2_3)Na(L^2_3Fe)]^-$: view from the side (upper) and along the Fe−Na−Fe axis (lower).

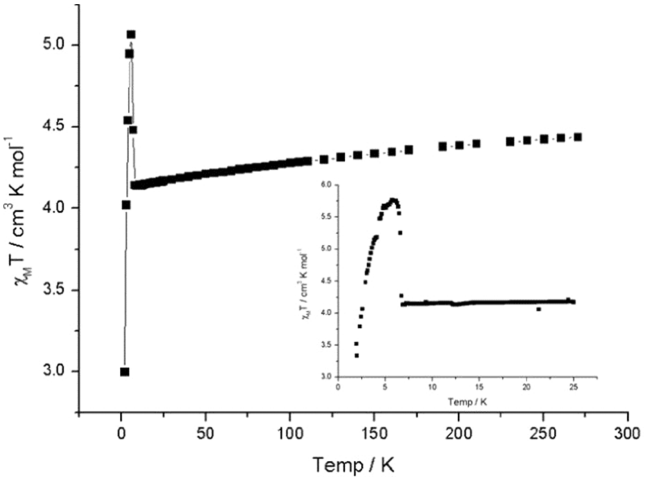

Figure 4. $\chi_M T$ vs T curves for $[Na(THF)_6][(MnL^2_3)Na(L^2_3Mn)]$ measured at 1000 Oe.

cm^3 K mol^{-1} at 5 K, indicating weak ferromagnetic coupling. This was confirmed by zero-field and field-cooled measurements (see SI). At lower temperatures still, $\chi_M T$ fell rapidly to 3.915 cm^3 K mol^{-1} at the base temperature. At 2 K, the material is magnetically saturated at 5 T with a value $M = 5\ \mu_B$ per Mn. This ferromagnetic behavior at lower temperatures could result from magnetic exchange between neighboring trimetallic anion units, and while this seems unlikely given the way in which the metal ions are tightly encapsulated, it did prompt us to consider deliberately connecting the metal centers together.

Complexes of L^3. This ligand provides a ready mechanism for intermolecular coordination of complex units to form network solids.

Treatment of HL^3 with sodium hydride in THF followed by $MnCl_2$ yielded a yellow suspension. The isolated solid was recrystallized from boiling THF; then crystals of polymeric $[Na(THF)_4][(MnL^3_3)Na(L^3_3Mn)]$ (30%) suitable for X-ray diffraction were grown slowly from THF/Et_2O. Similar reactions of Fe(II) did not give tractable products.

The repeat unit of $[Na(THF)_4][(MnL^3_3)Na(L^3_3Mn)]$ (Figure 5) contains the same type of trimetallic sandwich-like

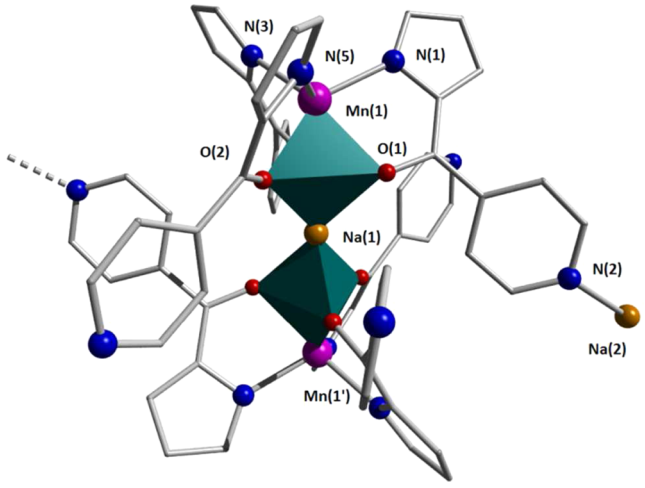

Figure 5. Repeat unit of chain complex $[Na(THF)_4][(MnL^3_3)Na(L^3_3Mn)]$. Selected bond lengths (Å): Mn(1)−N(1) 2.162(2), Mn(1)−N(3) 2.151(2), Mn(1)−N(5) 2.168(2), Mn(1)−O(1) 2.3405(16), Mn(1)−O(2) 2.2791(17), Mn(1)−Na(1) 3.2409(4), Na(1)−O(1) 2.3468(16), Na(1)−O(2) 2.3793(16), Na(2)−N(2). Selected bond angle (deg): Mn(1)−Na(1)−Mn(1′) 180. Solvents and hydrogen atoms are removed for clarity.

anion observed in the structures above for L^2. Here, however, the charge balancing Na(2) ions are *trans*-coordinated via one pyridine of each trischelate unit to form a 1D zigzag chain (Figure 6); the four remaining pyridine units are uncoordinated.

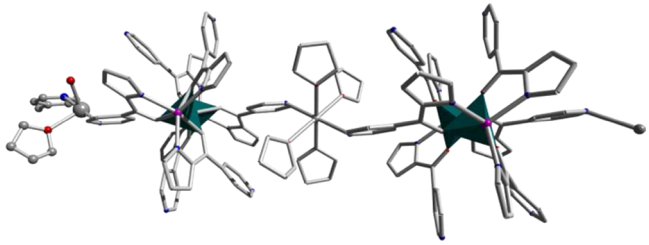

Figure 6. Zigzag chain structure of $[Na(THF)_4][(MnL^3_3)Na(L^3_3Mn)]$.

The sandwich anion units in this complex appear to be quite robust, and recrystallization of the solid from hot MeCN afforded orange crystals of $[Na(CH_3CN)_2][(MnL^3_3)Na(L^3_3Mn)]$ (63%). From crystallography, the anionic units (Figure 7) are similar to those in the THF solvate above, although the distance between Mn atoms is lower at 6.260 Å (cf. 6.482 Å). Four out of the six pyridine units in each anion are coordinated to the equatorial plane of bridging Na^+ ions,

DOI: 10.1021/om501218a
Organometallics 2015, 34, 2543−2549

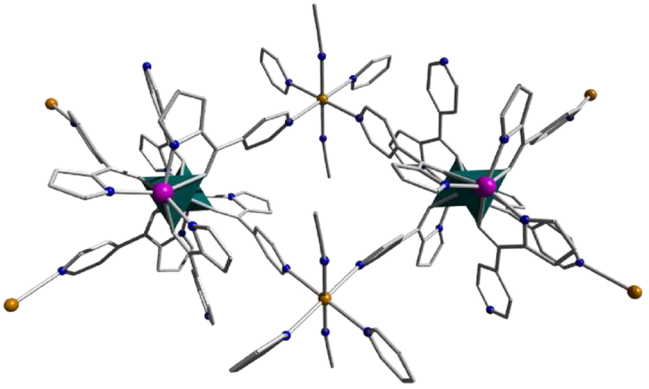

Figure 7. Structure of $[Na(CH_3CN)_2][(MnL^3{}_3)Na(L^3{}_3Mn)]$ showing intermolecular coordination of the Na^+ counterion.

with the coordination sphere of the latter made up by two additional MeCN ligands. The Na^+ centers and $[(MnL^3{}_3)Na(L^3{}_3Mn)]^-$ units are thus alternate nodes in a 2D network (Figure 8).

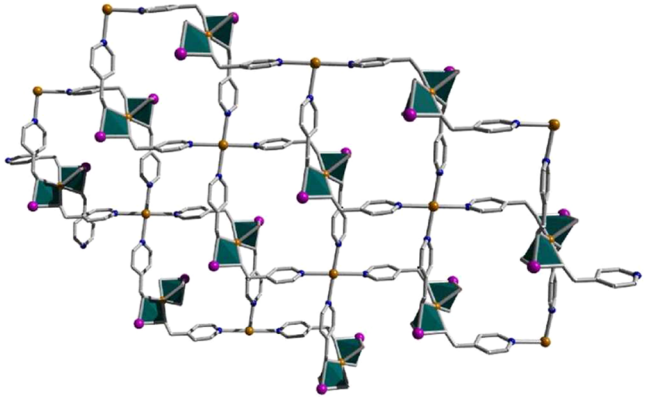

Figure 8. 2D grid topology produced in the solid state from $[Na(CH_3CN)_2][(MnL^3{}_3)Na(L^3{}_3Mn)]$ (pyrrolylcarbonyl units removed for clarity).

Despite the interion coordination modes for these Mn(II) complexes, the material was found to display only antiferromagnetic interactions (see SI).

The sandwich anions in the above structures are based on coordination of a large *fac*-$(ML^3{}_3)$ unit to Na^+. We thus set out to examine the effect of use of other group 1 cations on the structure. Potassium did not give tractable products, but treatment of HL^3 with LiOMe in dry methanol followed by the addition of a solution of $FeCl_2$ in methanol caused an immediate color change to blue then more slowly to purple. After 4 h a purple solid was present in a colorless solution. The apparently air-stable microcrystalline solid was collected by filtration (95%). While this isolated solid resisted fruitful recrystallization, single crystals suitable for X-ray diffraction were grown by slow diffusion of the starting materials. The solids gave very similar X-ray powder diffraction patterns, and microanalytical data were consistent with the formulation $[FeL^3{}_2]$ in both cases. ICP-MS analysis found that no lithium was incorporated.

As shown in Figure 9, the repeat unit contains one Fe center, which is coordinated by two bidentate N−O ligands L^3 and two pyridines from adjacent units. Overall the structure is very similar to that of a Schiff-base complex we described recently,[34]

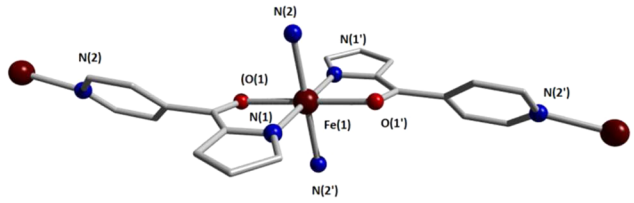

Figure 9. Repeat unit of complex $[FeL^3{}_2]_n$. Selected bond lengths (Å) and angles (deg): Fe(1)−N(1) 2.082(2), Fe(1)−O(1) 2.1585(15), Fe(1)−N(2) 2.1991(19), N(1)−Fe(1)−N(1′) 180.0, O(1)−Fe(1)−O(1′) 180.0, N(2)−Fe(1)−N(2′) 180.0, N(2)−Fe(1)− N(1′) 89.36(7), N(2)−Fe(1)−O(1) 87.45(6).

and relevant structural parameters are included in square brackets [thus] for comparison in the following description.

The geometry of the Fe unit is very close to octahedral with the two essentially coplanar chelates O(1)−Fe(1)−N(1) and O(1′)−Fe(1)−N(1′). These molecular units are assembled via pyridine coordination to give a planar rhombic array of Fe atoms (Figure 10) with Fe−Fe−Fe angles of 83.41° and 96.59°

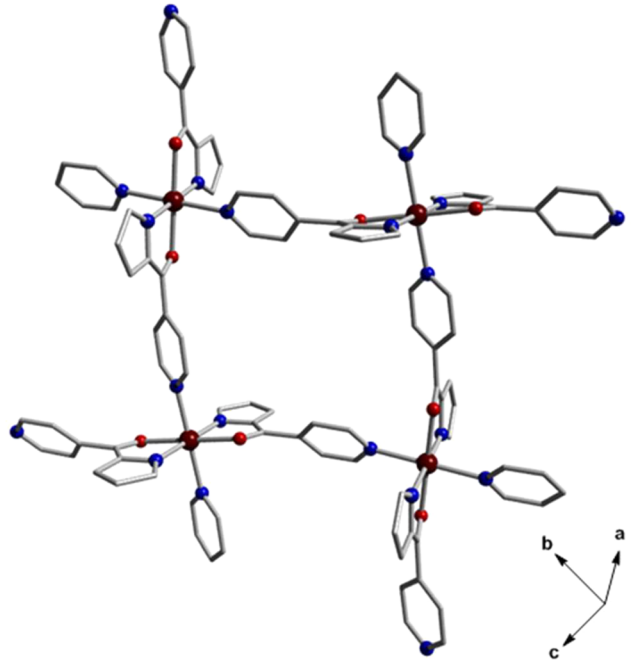

Figure 10. 2D orthogonal array of complex $[FeL^3{}_2]$.

[83.93° and 97.07°]. Nearest neighbor coordination units are arranged almost orthogonally at 84.22° [86.0°] with Fe···Fe distances of 9.135 Å [7.44 Å]. These *xy* planes all form an angle of ca. 81.24° [72.0°] to the Fe atom plane. The undulations of the organic ligands are accommodated efficiently by interdigitation, and no solvent is included, as confirmed by microanalysis.

The magnetic susceptibility data for $[FeL^3{}_2]$ (Figure 11) obey a Curie−Weiss law in the high-temperature regime (150−300 K), but $\chi_M T$ drops sharply from 3.610 cm^3 K mol^{-1} at 150 K to 0.678 cm^3 K mol^{-1} at 50 K, corresponding to spin-crossover (SCO) at 120 K. An additional drop at lower temperature occurs as a result of spin−orbit coupling.

The complex $[MnL^3{}_2]$ was prepared in high yield in a similar manner to the Fe complex, and while we were unable to grow

DOI: 10.1021/om501218a
Organometallics 2015, 34, 2543−2549

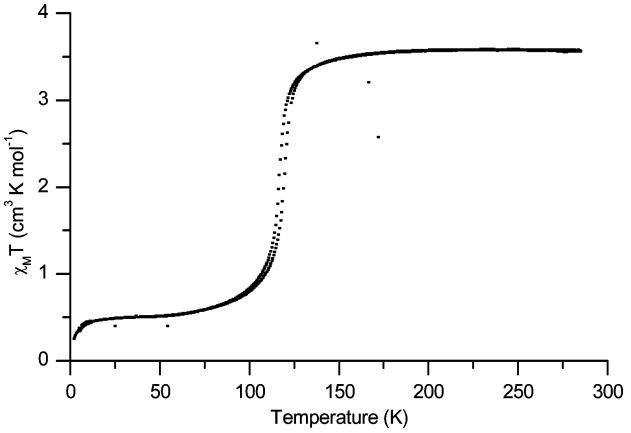

Figure 11. Magnetic moment vs T for $[FeL^3_2]$ at 1000 Oe.

single crystals, we note that the two complexes have very similar powder X-ray diffraction patterns and IR spectra.

CONCLUSIONS

The 2-amide ligand $\mathbf{L^1}$ did not support M(II) (M = Mn, Fe) complexes in this study, presumably because it is the stronger π-donor in the series. Correspondingly, the aroyl derivatives $\mathbf{L^2}$ and $\mathbf{L^3}$ gave M(II) compounds.

Of particular interest in these compounds is the anionic structure formed by coordination of two scorpionate-like *fac*-(ML_3) units to a central Na^+, present in every structure of this metal. This sandwich structure suggested that it may be possible to synthesize systems containing three transition metal ions via salt metathesis, i.e., $[(ML_3)M'(L_3M)]$. These might have interesting magnetic properties or be probes for electron transfer in mixed valence species.

When Li salts are used in the $\mathbf{L^3}$ reactions, the scorpionate sandwich anions are not formed, and instead 2D layer rhombic structures are produced. The very readily synthesized complex $[FeL^3_2]$ exhibits SCO at ca. 120 K.

The ketopyrrolyl system exemplified by $\mathbf{L^2}$ and $\mathbf{L^3}$ promises to be readily modified. No doubt Lappert would consider introducing a much bulkier benzoyl unit, which would prevent formation of the interdigitated sandwich structure and thus open up new metal-based reactivity. On the basis of the different behaviors of $\mathbf{L^1}$ and $\mathbf{L^2}$, we would also suggest that the electronic properties could be modified by *p*-substitution at the arene, noting in this context Reglinski's work on soft scorpionates.[35] The synthetic route to $\mathbf{L^2}$ also allows use of different pyrroles.

By judicious choice of substituent patterns and reagents it should thus be possible to open up a readily accessible 2-ketopyrrolylamido chemistry.

EXPERIMENTAL SECTION

General Considerations. Solvents and chemicals were purchased from commercial sources (Sigma-Aldrich, Acros, Lancaster, Fisher Scientific, Alfa Aesar, or Strem) and used without further purification unless otherwise stated. (1*H*-Pyrrol-2-yl)(pyrrolidin-1-yl)methanone (HL^1)[30] and (1*H*-pyrrol-2-yl)(pyrrolidin-1-yl)methanone (HL^2)[31] were made by literature routes.

Sodium hydride dispersion in mineral oil was placed in a Schlenk vessel under argon and washed three times with dry diethyl ether to remove the oil. The solid was then dried and stored in the glovebox.

Procedures were generally carried out under argon by using a dual manifold vacuum/argon line and standard Schlenk techniques or an MBraun drybox. Dried solvents were made by refluxing for 3 d under dinitrogen over the appropriate drying agents (potassium for THF; sodium−potassium alloy for diethyl ether; magnesium methoxide for methanol; calcium hydride for acetonitrile) and degassed before use. THF and diethyl ether were additionally predried over sodium wire. Solvents were stored in glass ampules under argon. All glassware and cannulae were stored in an oven (>373 K).

NMR spectra were recorded on a DPX-400 spectrometer, and the spectra were referenced internally using residual protio solvent resonances relative to tetramethylsilane (δ = 0 ppm). ESI mass spectra were recorded on a Bruker Esquire2000. Infrared spectra were obtained either as Nujol mulls using a PerkinElmer 100 FTIR spectrometer or directly using a Nicolet FTIR instrument. Elemental analyses were performed by Warwick Analytical Services or Medac Analytical Ltd., Surrey, UK. Ultraviolet/visible spectra were obtained as an appropriate solution in a quartz cell of path length 1 cm, using a Jasco V-660 spectrometer.

Magnetization measurements were made as a function of temperature (T) and applied magnetic field (H) using a Quantum Design MPMS-5 SQUID magnetometer. Samples were randomly oriented powders placed in Kel-F capsules. The capsule was centered using a pure Ni sample. The data were corrected for the measured diamagnetism of the capsule and the diamagnetic contributions of the sample using Pascal's constants.[36]

Crystallography. Single-crystal X-ray diffraction data were collected on an Oxford Diffraction Gemini four-circle system with a Ruby CCD area detector at Warwick or on a Bruker Nonius KappaCCD diffractometer system at UK National Crystallography Service (NCS).[37] Crystals were coated in inert oil prior to transfer to a cold nitrogen gas stream on the machine. The temperature of crystals was controlled using an Oxford Cryosystem Cobra. Using the SHELXTL suite,[38] the structure was solved with the ShelXS[38] structure solution program using direct methods and refined with the ShelXL[38] refinement package using least squares minimization.

For the structure of $[Na(THF)_4][(MnL^3_3)Na(L^3_3Mn)]$ the asymmetric unit contains one-third of a complex cation $[Na(THF)_6]^+$ and anion $[(FeL^2_3)Na(L^2_3Fe)]^-$ both lying on a 3-fold inversion axis. The anion was modeled as disordered over two positions related by a twist about the 3-fold axis and refines to a ratio of 58:42. One THF molecule in the asymmetric unit was modeled as disordered over three positions roughly related by rotations about the Na−O THF bond. These were refined with a SUMP command in SHELX, restraining their combined occupancy to 1. At later stages of the refinement, these occupancies were fixed at 40:35:25. Many restraints were used to give these molecules reasonable bonds, angles (SAME), and thermal parameters (SIMU). The disordered THF was refined isotropically. A small amount of electron density centered around a 3-fold axis was simply modeled as two partially occupied carbon atoms C100 and C101 refined at 0.2 occupancy. Due to the low occupancy and high symmetry, it was not possible to resolve this into any chemically reasonable molecule or fragment. There was no great improvement in the R value using the Squeeze-modified HKL file.

Isonicotinoyl Chloride Hydrochloride.[39] Isonicotinic acid (20.0 g, 162 mmol) was suspended in dry toluene (150 mL) in a round-bottom Schlenk vessel at 0 °C. Oxalyl chloride (28.3 mL, 324 mmol) was added slowly via syringe. After 1 h the reaction was left to warm to ambient temperature and was stirred overnight. The product was collected by cannula filtration, washed with dry toluene (100 mL), and dried *in vacuo*. Yield: 18.2 g, 63%. ^{1}H NMR (400 MHz, 298 K, DMSO): δ_H 8.90 (2H, dd, J = 1.5, 5 Hz), 8.03 (2H, dd, J = 1.5, 5 Hz). ^{13}C{^{1}H} NMR (100 MHz, 298 K, DMSO): δ_C 164.5 (C═O), 146.0 (Py), 144.1 (Py), 126.8 (Py). Anal. Found (calcd for $C_6H_3Cl_2NO$): C 40.54 (40.48), H 2.94 (2.83), N 7.72 (7.87).

Pyridin-4-yl(1*H*-pyrrol-2-yl)methanone (HL^3). A dry round-bottom Schlenk vessel charged with aluminum chloride (3.34 g, 25.0 mmol, 2.5 equiv) was flushed with argon, and dry DCM (100 mL) was added. The mixture was stirred for 30 min before isonicotinoyl chloride hydrochloride (1.78 g, 10.0 mmol) was added. After 2 h, pyrrole (1.34 g, 1.39 mL, 20.0 mmol) was added. The reaction mixture was stirred under argon overnight at ambient temperature. The flask

DOI: 10.1021/om501218a
Organometallics 2015, 34, 2543−2549

was cooled to 0 °C using an ice−water bath before saturated aqueous $NaHCO_3$ was added slowly with stirring until the pH of the aqueous layer was 8.0. The aluminum byproduct precipitate was removed by filtration through a Celite filter aid. The product was extracted into chloroform (5 × 75 mL) and dried over sodium sulfate, and the solvent was removed under reduced pressure to leave the crude product. Purification by column chromatography (ethyl acetate/hexane, 2:1) yielded a pale yellow crystalline solid. Yield = 1.38 g, 8.0 mmol, 80%.

^{1}H NMR (400 MHz, 298 K, $CDCl_3$): δ_H 9.88 (br s, 1H, Pyr-N*H*), 8.80 (2H, dd, 4.5, 1.5 Hz), 7.69 (2H, dd, 4.5, 1.5 Hz), 7.22 (1H, m), 6.89 (1H, m), 6.37 (1H, m). ^{13}C{^{1}H} NMR (100 MHz, 298 K, $CDCl_3$): δ_C 182.9 (C═O), 150.3, 145.0, 130.5, 126.6, 122.3, 120.3, 111.6. MS (ESI): m/z 171.2 $(M - H)^-$. IR: ν cm^{-1} 3115 w, 3063 w, 3026 w, 2989 w, 2921 w, 2875 w, 2801 w, 2683 w, 1612 m, 1600 m, 1542 m, 1465 w, 1427 m, 1412 m, 1392 s, 1342 m, 1320 m, 1263 w, 1220 m, 1197 w, 1140 m, 1093 m, 1064 w, 1045 m, 1002 m, 986 w, 962 w, 887 m, 866 m, 834 m, 792 s, 757 m, 738 s, 723 s. Anal. Found (calcd for $C_{10}H_8N_2O$): C 69.67 (69.76), H 4.38 (4.68), N 16.32 (16.27).

[MnL^1_3]. HL^1 (0.516 g, 3.14 mmol) was stirred with NaH (0.086 g, 3.6 mmol) in dry THF (20 mL) for 15 min. The resulting yellow solution was transferred via cannula into a solution of $MnCl_2$ (0.126 g, 1.0 mmol) in dry THF (20 mL) at room temperature. The solution turned gray immediately. The reaction mixture was stirred overnight at ambient temperature. The solution was filtered, and the volume of the solution was reduced by half before Et_2O (5 mL) was added to induce crystallization. A few crystals of the complex were isolated by filtration and washed with a little cold THF. Single crystals were grown from the solution of THF/Et_2O (3:1).

Crystallography. $C_{27}H_{33}MnN_6O_3$, M = 544.53, monoclinic, a = 9.7037(12) Å, b = 17.001(2) Å, c = 15.6962(13) Å, α = 90.00°, β = 100.350(7)°, γ = 90°, V = 2547.4(5) Å^3, T = 100(2) K, space group $P2_1/n$, Z = 4, 19 043 reflections measured, 4910 independent reflections (R_{int} = 0.0672). The final R values were R_1 = 0.0907 ($I > 2\sigma(I)$), $wR(F^2)$ 0.1635 ($I > 2\sigma(I)$), R_1 (all data) = 0.1372, $wR(F^2)$ (all data) = 0.1901.

[FeL^1_3]. This was prepared in the same manner as [MnL^1_3], from anhydrous $FeCl_2$. A few single crystals were grown from THF/Et_2O (3:1).

Crystallography. $C_{27}H_{33}FeN_6O_3$, M = 545.44, monoclinic, a = 9.99697(15) Å, b = 31.4459(4) Å, c = 16.9520(2) Å, α = 90.00°, β = 103.4800(15)°, γ = 90°, V = 5182.28(13) Å^3, T = 100(2) K, space group $P2_1/n$, Z = 8, 58 787 reflections measured, 9984 independent reflections (R_{int} = 0.0619). The final R values were R_1 = 0.0413 ($I > 2o(I)$), $wR(F^2)$ = 0.0985 ($I > 2o(I)$), R_1 (all data) = 0.0498, $wR(F^2)$ (all data) = 0.1038.

[Na(THF)$_6$][(FeL^2_3)Na(L^2_3Fe)]. HL^2 (0.513 g, 3.0 mmol) was stirred with NaH (0.086 g, 3.6 mmol, 1.2 equiv) in dry THF (20 mL) for 15 min. The resulting yellow solution was transferred via cannula into a solution of $FeCl_2$ (0.127 g, 1.0 mmol) in dry THF (20 mL) at ambient temperature. The deep red solution was stirred overnight and was filtered via cannula. Large red blocks grew at 4 °C over 1 week (0.259 g, 32%).

IR (cm^{-1}): 2911 vs, 2850 vs, 1601 w, 1581 w, 1463 vs, 1377 vs, 1282 m, 1126 m, 1040 m, 905 m, 880 m, 794 w, 754 m, 731 s, 700 m. Anal. Found (calcd for $C_{90}H_{96}Fe_2N_6Na_2O_{12}$): C 67.37 (67.08), H 6.38 (6.00), N 5.32 (5.22). UV in THF (λ/nm; ε/M^{-1} cm^{-1}): 244 (30 000), 302 (48 000).

Crystallography. $C_{90}H_{96}Fe_2N_6Na_2O_{12}$, M = 1611.41, hexagonal, a = 13.11870(10) Å, b = 13.11870(10) Å, c = 28.3181(5) Å, α = 90.00°, β = 90.00°, γ = 120.00°, V = 4220.62(9) Å^3, T = 100(2) K, space group $P\bar{3}_1$ c, Z = 2, 48 829 reflections measured, 2708 independent reflections (R_{int} = 0.0513). The final R values were R_1 = 0.0843 ($I > 2\sigma(I)$), $wR(F^2)$ = 0.2421 ($I > 2\sigma(I)$), R_1 (all data) = 0.0937, $wR(F^2)$ (all data) = 0.2536.

[Na(THF)$_6$][(MnL^2_3)Na(L^2_3Mn)]. This was synthesized from $MnCl_2$ in a similar manner to the Fe analogue. Large yellow blocks were grown from diethyl ether at room temperature over 2 h and were isolated by decantation (0.420 g, 52%).

Anal. Found (calcd for $C_{90}H_{96}Mn_2N_6Na_2O_{12}$): C 66.77 (67.16), H 6.38 (6.01), N 5.32 (5.22). IR (cm^{-1}): 2925 vs, 2854 vs, 1602 w, 1584 m, 1464 vs, 1377 vs, 1282 m, 1196 m, 1172 w, 1095 w, 1044 m, 988 w, 905 m, 880 m, 795 w, 754 m, 730 s, 699 m, 681 w. UV in THF (λ/nm; ε/M^{-1} cm^{-1}): 244 (76 000), 302 (125 000).

[Na(THF)$_4$][(MnL^3_3)Na(L^3_3Mn)]·2THF·Et$_2$O. HL^3 (0.516 g, 3.0 mmol) was stirred with NaH (0.086 g, 3.6 mmol) in dry THF (20 mL) for 15 min. The resulting yellow solution was transferred via cannula into a solution of $MnCl_2$ (0.126 g, 1.0 mmol) in dry THF (20 mL) at room temperature. After stirring overnight, the yellow mixture was heated to reflux until the yellow solid dissolved. The resulting solution was filtered hot via cannula and allowed to cool. Diethyl ether was added to the onset of crystallization, and the mixture left to stand, giving yellow single crystals (0.25 g, 30%).

Anal. Found (calcd for $C_{88}H_{100}Mn_2N_{12}Na_2O_{13}$): C 62.37 (62.55), H 5.78 (5.97), N 9.62 (9.95). IR (cm^{-1}): 3083 w, 3062 w, 1603 w, 1561 s, 1525 vs, 1498 m, 1479 m, 1437 m, 1428 m, 1406 m, 1319 w, 1271 vs, 1214 w, 1192 s, 1071 w, 1063 w, 1045 s, 1031 vs, 985 m, 906 m, 893 s, 881 m, 837 s, 749 vs, 732 vs, 683 vs, 666 w. UV in THF (λ, nm; ε, M^{-1} cm^{-1}): 266 (27 000), 312 (44 000), 365 (24 000).

Crystallography. $C_{88}H_{100}Mn_2N_{12}Na_2O_{13}$, M = 1689.66, triclinic, a = 12.4104(6) Å, b = 13.3080(6) Å, c = 15.0872(6) Å, α = 104.434(3)°, β = 102.056(4)°, γ = 111.251(4)°, V = 2121.9(2) Å^3, T = 100(2) K, space group $P\bar{1}$, Z = 1, 16 045 reflections measured, 8012 independent reflections (R_{int} = 0.0345). The final R values were R_1 = 0.0528 ($I > 2o(I)$), $wR(F^2)$ = 0.1380 ($I > 2o(I)$), R_1 (all data) = 0.0583, $wR(F^2)$ (all data) = 0.1432.

[Na(MeCN)$_2$][(MnL^3_3)Na(L^3_3Mn)]·MeCN. NaL^3 (3.0 mmol) and $MnCl_2$ (0.126 g, 1.0 mmol) were stirred overnight in dry THF (20 mL) as above. The solvent was removed *in vacuo*, and the product was extracted into MeCN (30 mL) with heating. The volume of the red MeCN solution was reduced by half to induce crystallization. Yield: 0.41 g, 63%. Further single crystals were grown from the solution upon standing at 4 °C for 1 week.

IR (cm^{-1}): 3065 w, 1601 w, 1560 s, 1526 vs, 1495 m, 1480 m, 1429 m, 1407 w, 1318 w, 1270 vs, 1215 w, 1194 s, 1089 w, 1071 w, 1045 m, 1030 vs, 985 m, 905 w, 894 s, 836 s, 749 vs, 732 vs, 682 vs, 666 w. Anal. Found (calcd for $C_{66}H_{51}Mn_2N_{15}Na_2O_6$): C 60.47 (60.69), H 4.18 (3.94), N 16.32 (16.09). UV in MeCN (λ, nm; ε, M^{-1} cm^{-1}): 265 (24 000), 260 (40 000), 306 (22 600).

Crystallography. $C_{66}H_{51}Mn_2N_{15}Na_2O_6$, M = 1306.08, triclinic, a = 10.3060(4) Å, b = 12.9626(4) Å, c = 13.0826(6) Å, α = 63.489(4)°, β =80.865(4)°, γ = 80.113(3)°, V = 1534.05(11) Å^3, T = 100(2) K, space group $P\bar{1}$, Z = 1, 15 296 reflections measured, 5867 independent reflections (R_{int} = 0.0365). The final R values were R_1 = 0.0403 ($I > 2o(I)$), $wR(F^2)$ = 0.0992 ($I > 2o(I)$), R_1 (all data) = 0.0433, $wR(F^2)$ (all data) = 0.1020.

[FeL^3_2]. HL^3 (0.344 g, 2.0 mmol) was stirred with MeOLi (0.091 g, 2.4 mmol) in dry MeOH (20 mL) for 15 min. This resulted in a yellow solution, to which was added a solution of $FeCl_2$ (0.127 g, 1.0 mmol) in dry MeOH (15 mL) via canuula. The solution turned blue and then purple after 1 h. The mixture was stirred overnight at ambient temperature. The purple product was collected by filtration and dried *in vacuo* for 4 h (0.378 g, 95%). Single crystals were grown in an NMR tube from a slow diffusion of two layered solutions of starting materials in MeOH solution (ca. 1.0 M).

Anal. Found (calcd for $C_{20}H_{14}FeN_4O_2$: C 60.37 (60.33), H 3.38 (3.54), N 14.32 (14.07). IR (cm^{-1}): 3058 w, 1610 m, 1559 s, 1524 vs, 1497 m, 1434 m, 1415 w, 1388 vs, 1317 w, 1278 m, 1221 w, 1196 m, 1139 w, 1046 m, 993 m, 909 m, 880 m, 852 m, 748 s, 726 vs, 693 vs. Due to the insolubility of the material, we were unable to collect UV data.

Crystallography. $C_{20}H_{14}FeN_4O_2$, M = 398.20, monoclinic, a = 7.7538(2) Å, b = 13.6404(4) Å, c = 8.2758(3) Å, α = 90.00°, β = 98.581(3)°, γ = 90.00°, V = 865.49(5) Å^3, T = 100(2) K, space group $P2(1)/n$, Z = 2, 3844 reflections measured, 1525 independent reflections (R_{int} = 0.0249). The final R values were R_1 = 0.0412 ($I > 2\sigma(I)$), $wR(F^2)$ = 0.1147 ($I > 2\sigma(I)$), R_1 (all data) = 0.0441, $wR(F^2)$ (all data) = 0.1189.

DOI: 10.1021/om501218a
Organometallics 2015, 34, 2543−2549

[MnL$^3_2$]. This was prepared as the Fe analogue, from $MnCl_2$ (0.126 g, 1.0 mmol). Yield: 0.381 g, 96%. IR (cm^{-1}): 3057 w, 1611 m, 1559 s, 1523 vs, 1497 m, 1437 m, 1388 vs, 1317 w, 1278 w, 1196 m, 1140 w, 1046 m, 991 m, 907 m, 880 m, 852 m, 748 s, 726 vs, 694 vs. Anal. Found (calcd for $C_{20}H_{14}MnN_4O_2$): C 60.47 (60.46), H 3.38 (3.55), N 14.32 (14.10). Due to the insolubility of the material, we were unable to collect UV data.

■ ASSOCIATED CONTENT

Supporting Information

CIF files for all structures, additional magnetic measurement data. The Supporting Information is available free of charge on the ACS Publications website at DOI: 10.1021/om501218a.

■ AUTHOR INFORMATION

Corresponding Author

*E-mail: peter.scott@warwick.ac.uk.

Notes

The authors declare no competing financial interest.

■ ACKNOWLEDGMENTS

We thank the University of Warwick for a Warwick Postgraduate Research Fellowship (L.L.). The Oxford Diffraction Gemini XRD system was obtained through the Science City Advanced Materials project: Creating and Characterizing Next Generation Advanced Materials project, with support from Advantage West Midlands (AWM) and partially funded by the European Regional Development Fund (ERDF).

■ DEDICATION

P.S. dedicates this work to the memory of his colleague at Sussex, Mike Lappert, who gave him much encouragement in his early career.

■ REFERENCES

(1) Hitchcock, P. B.; Lappert, M. F.; Wang, Z.-X. *J. Organomet. Chem.* **2008**, *693*, 3767−3770.
(2) Avent, A. G.; Hitchcock, P. B.; Lappert, M. F.; Sablong, R.; Severn, J. R. *Organometallics* **2004**, *23*, 2591−2600.
(3) Gehrhus, B.; Hitchcock, P. B.; Lappert, M. F.; Heinicke, J.; Boese, R.; Blaser, D. *J. Organomet. Chem.* **1996**, *521*, 211−220.
(4) Hitchcock, P. B.; Lappert, M. F.; Protchenko, A. V. *Chem. Commun.* **2005**, 951−953.
(5) Deelman, B.-J.; Hitchcock, P. B.; Lappert, M. F.; Lee, H.-K.; Leung, W.-P. *J. Organomet. Chem.* **1996**, *513*, 281−285.
(6) Hitchcock, P. B.; Khvostov, A. V.; Lappert, M. F.; Protchenko, A. V. *Dalton Trans.* **2009**, 2383−2391.
(7) Hitchcock, P. B.; Lappert, M. F.; Liu, D.-S. *J. Chem. Soc., Chem. Commun.* **1994**, 2637−2638.
(8) Hitchcock, P. B.; Khvostov, A. V.; Lappert, M. F.; Protchenko, A. V. *Dalton Trans.* **2009**, 2383−2391.
(9) Hitchcock, P. B.; Lappert, M. F.; Liu, D.-S. *J. Chem. Soc., Chem. Commun.* **1994**, 1699−1700.
(10) Bourget-Merle, L.; Lappert, M. F.; Severn, J. R. *Chem. Rev.* **2002**, *102*, 3031−3066.
(11) Piers, W. E.; Emslie, D. J. H. *Coord. Chem. Rev.* **2002**, *233*, 131−155.
(12) LeBlanc, F. A.; Piers, W. E.; Parvez, M. *Angew. Chem., Int. Ed.* **2014**, *53*, 789−792.
(13) Trofymchuk, O. S.; Gutsulyak, D. V.; Quintero, C.; Parvez, M.; Daniliuc, C. G.; Piers, W. E.; Rojas, R. S. *Organometallics* **2013**, *32*, 7323−7333.
(14) Chu, T.; Piers, W. E.; Dutton, J. L.; Parvez, M. *Organometallics* **2012**, *32*, 1159−1165.
(15) Chong, E.; Brandt, J. W.; Schafer, L. L. *J. Am. Chem. Soc.* **2014**, *136*, 10898−10901.
(16) Garcia, P.; Lau, Y. Y.; Perry, M. R.; Schafer, L. L. *Angew. Chem., Int. Ed.* **2013**, *52*, 9144−9148.
(17) Leitch, D. C.; Platel, R. H.; Schafer, L. L. *J. Am. Chem. Soc.* **2011**, *133*, 15453−15463.
(18) Keane, A. J.; Yonke, B. L.; Hirotsu, M.; Zavalij, P. Y.; Sita, L. R. *J. Am. Chem. Soc.* **2014**, *136*, 9906−9909.
(19) Keane, A. J.; Zavalij, P. Y.; Sita, L. R. *J. Am. Chem. Soc.* **2013**, *135*, 9580−9583.
(20) Wei, J.; Hwang, W.; Zhang, W.; Sita, L. R. *J. Am. Chem. Soc.* **2013**, *135*, 2132−2135.
(21) Chomitz, W. A.; Arnold, J. *Inorg. Chem.* **2009**, *48*, 3274−3286.
(22) Schmidt, J. A. R.; Arnold, J. *Organometallics* **2002**, *21*, 2306−2313.
(23) Matsui, S.; Yoshida, Y.; Takagi, Y.; Spaniol, T. P.; Okuda, J. *J. Organomet. Chem.* **2004**, *689*, 1155−1164.
(24) Mirebeau, J.-H.; Le Bideau, F.; Marrot, J.; Jaouen, G. *Organometallics* **2008**, *27*, 2911−2914.
(25) Carabineiro, S. A.; Gomes, P. T.; Veiros, L. F.; Freire, C.; Pereira, L. C. J.; Henriques, R. T.; Warren, J. E.; Pascu, S. I. *Dalton Trans.* **2007**, 5460−5470.
(26) Reardon, D.; Guan, J.; Gambarotta, S.; Yap, G. P. A.; Wilson, D. R. *Organometallics* **2002**, *21*, 4390−4397.
(27) Jazzar, R. F. R.; Varrone, M.; Burrows, A. D.; Macgregor, S. A.; Mahon, M. F.; Whittlesey, M. K. *Inorg. Chim. Acta* **2006**, *359*, 815−820.
(28) Rubino, S.; Petruso, S.; Pierattelli, R.; Bruno, G.; Stocco, G. C.; Steardo, L.; Motta, M.; Passerotto, M.; Giudice, E. D.; Gulì, G. *J. Inorg. Biochem.* **2004**, *98*, 2071−2079.
(29) Hart, J. S.; Nichol, G. S.; Love, J. B. *Dalton Trans.* **2012**, *41*, 5785−5788.
(30) Donohoe, T. J.; Guyo, P. M.; Beddoes, R. L.; Helliwell, M. *J. Chem. Soc., Perkin Trans. 1* **1998**, 667−676.
(31) White, J.; McGillivray, G. *J. Org. Chem.* **1977**, *42*, 4248−4251.
(32) Howson, S. E.; Allan, L. E. N.; Chmel, N. P.; Clarkson, G. J.; van Gorkum, R.; Scott, P. *Chem. Commun.* **2009**, 1727−1729.
(33) Sebli, C. P.; Howson, S. E.; Clarkson, G. J.; Scott, P. *Dalton Trans.* **2010**, *39*, 4447−4454.
(34) Li, L.; Clarkson, G. J.; Evans, D. J.; Lees, M. R.; Turner, S. S.; Scott, P. *Chem. Commun.* **2011**, *47*, 12646−12648.
(35) Reglinski, J.; Spicer, M. D. *Coord. Chem. Rev.* **2015**, DOI: 10.1016/j.ccr.2015.02.023.
(36) Bain, G. A.; Berry, J. F. *J. Chem. Educ.* **2008**, *85*, 532−536.
(37) Coles, S. J.; Gale, P. A. *Chem. Sci.* **2012**, *3*, 683−689.
(38) Sheldrick, G. M. *Acta Crystallogr., Sect. A* **2008**, *64*, 112−122.
(39) Nättinen, K. I.; Rissanen, K. *Cryst. Growth Des.* **2003**, *3*, 339−353.

DOI: 10.1021/om501218a
Organometallics 2015, 34, 2543−2549